



Synthesis, characterization, biological screening and molecular docking of Zn(II) and Cu(II) complexes of 3,5-dichlorosalicylaldehyde-N⁴-cyclohexylthiosemicarbazone

Nimya Ann Mathews¹ | P.M. Sabura Begum¹ | M.R. Prathapachandra Kurup^{1,2}

¹Department of Applied Chemistry, Cochin University of Science and Technology, Kochi 682 022 Kerala, India

²Department of Chemistry, School of Physical Sciences, Central University of Kerala, Tejaswini Hills, Periyar, Kasaragod 671 320, India

Correspondence

M. R. Prathapachandra Kurup, Department of Chemistry, School of Physical Sciences, Central University of Kerala, Tejaswini Hills, Periyar, Kasaragod, 671 320, India.
Email: mrpcusat@gmail.com

Funding information

University Grants Commission, Grant/Award Number: Nov 2017-111132

A 3,5-dichlorosalicylaldehyde-N⁴-cyclohexylthiosemicarbazone (C₁₄H₁₆Cl₂N₃OS) and its complexes [Zn(dsct)(phen)]·DMF (**1**), [Zn(dsct)(bipy)]·DMF (**2**), [Cu(dsct)(bipy)]·DMF (**3**) (phen = 1,10-phenanthroline, bipy = 2,2'-bipyridine) were synthesized and characterized by CHN analysis, FT-IR, UV-vis and NMR spectra. The molecular structure of the thiosemicarbazone (H₂dsct) and its complexes have been resolved using single crystal XRD studies. In the complexes, thiosemicarbazone exist in the thioiminolate form and acts as dideprotonated tridentate ligand coordinating through phenolic oxygen, thioiminolate sulfur and azomethine nitrogen. The antibacterial activity of the prepared compounds were screened against *Escherichia coli*, *Salmonella typhi*, *Enterobacter aerogenes*, *Shigella dysenteriae*, *Bacillus cereus*, *Staphylococcus aureus*. All the complexes showed activity against bacterial strains *E.coli* and *Salmonella typhi*. The thiosemicarbazone showed activity against three bacterial strains such as *E. coli*, *Enterobacter aerogenes* and *Shigella dysenteriae*. Complex **2** showed very good antibacterial activity as compared to standard drug (Ampicillin) against the bacterial strain, *Salmonella typhi*. Finally, the thiosemicarbazone and its complexes have been used to accomplish molecular docking studies against an Epidermal Growth Factor Receptor (EGFR) and breast cancer mutant 3hb5-oxidoreductase to determine the most preferred mode of interaction. The results confirm that the complex [Cu(dsct)(bipy)]·DMF(**3**) showed the highest docking score as compared to other complexes under study. The [Cu(dsct)(bipy)]·DMF(**3**) complex was evaluated for their anticancer activities against breast cancer cell line (MCF-7) and normal L929 (Mouse Fibroblast) cell line. It was found that the compound showed an LC₅₀ of 6.25 µg/mL against breast cancer cell line (MCF-7).

KEYWORDS

antibacterial activity, crystal structures, molecular docking, MTT, Thiosemicarbazones

1 | INTRODUCTION

Thiosemicarbazones are a class of Schiff base compound of chelating bio ligands that contain a thiourea moiety and they attract considerable attention due to their ease of

preparation, excellent complexation, variety of coordination modes and useful pharmacological properties and pharmacological applications.^[1,2] They are versatile ligands and efficient metal chelators. A number of reasons have been responsible for the versatility in their

coordination, such as, intramolecular hydrogen bonding, bulkier coligands, steric crowding on the azomethine carbon atom and π - π stacking interaction. They act as chelating ligand with certain metal ions, by bonding with the sulfur and hydrazine nitrogen atoms. They are also versatile ligands which can coordinate in both their neutral^[3] and anionic forms.^[4] They are a privileged ligands with their ability to create complexes with wide range of transition metal ions yielding stable and strongly coloured metal complexes.^[5] Different variety of thiosemicarbazone derivatives have been synthesized as antibacterial, antiviral, antifungal, antioxidant, anti-inflammatory and antiproliferative agents.^[6-9] It is found that Cu (II) complexes with heterocyclic ligand show biological activity.^[10] The nitrogen and sulfur donor atoms present in the thiosemicarbazone might be the reason for its potential biological activity.^[11] Recently Ayman *et al.* reported antibacterial studies of newly synthesized cobalt (II, III), nickel (II) and copper (II) complexes with salicylaldehyde N⁴-antipyrinylthiosemicarbazone^[9b]. 3-Aminopyridine-2-carboxaldehyde thiosemicarbazone (triapine) has been the most studied thiosemicarbazone which has entered phase II clinical trials as a chemotherapeutic agent.^[12,13] But it ended up with side effects.

Molybdenum complexes of salicylaldehyde thiosemicarbazones show *in vitro* DNA binding along with antitumour activity.^[14] Biological activities of complexes like DNA binding, antibacterial and cytotoxic activities of Ni(II) complexes of substituted salicylaldehyde thiosemicarbazones were well explored.^[15,16] Kalairasi *et al.* reported a Ni (II) complex of an ONS donor thiosemicarbazones as an antiproliferate towards MCF-7 and HeLa cell lines.^[17]

In this paper, our attention is directed to the design of Zn(II) and Cu(II) complexes of a thiosemicarbazone with heterocyclic bases as secondary ligands. Structures of many biomolecules contain copper and zinc ions, which are essential for their function.^[18] The design of the pro ligand is important for synthesis of more effective drugs with less side effects. Copper complexation with thiosemicarbazone was an effective anticancer strategy. Studies have revealed that the introduction of planar aromatic N-containing ligands such as bipyridine and its derivatives that are similar to the purine and pyrimidine bases can produce complexes with promising properties for the design and development of drugs due to their potential to interact with DNA and proteins.^[19]

Nowadays, cancer is undoubtedly the most alarming threat faced by humanity and one of the primary targets relating to the medicinal chemistry. The most frequently used treatments for breast cancer and other cancers till date is chemotherapy. But along with the affected cells, normal proliferating cells are also getting destroyed by

this treatment. Hence there is an emerging need to identify new drugs that are effective and safe for the treatment of cancers. The copper and zinc complexes of thiosemicarbazones are a class of compounds with medicinal property had reported earlier in 1960s. Very lately, a copper complex [Cu^{II} (pyrimol)Cl] have been reported by Reedijk and co-workers which is cytotoxic towards L1210 murine leukaemia and A2780 human ovarian carcinoma cell line.^[20] Palaniandavar, Chakravarty, Von and their co-workers reported the function of hydrophobicity of ligands in many ternary copper(II) complexes, which results in DNA binding and cleavage and induce apoptosis in various cancer cell lines.^[21] Bearing in mind that ONS donor system is a common feature for all the compounds with carcinostatic potency, we have carried out molecular docking on the synthesized compounds with receptor of breast cancer (3hb5) and EGFR TK (1 m17) and also the cytotoxic studies of the complex using MTT assay.

2 | EXPERIMENTAL SECTION

2.1 | Materials

Cyclohexylisothiocyanate (Alfa Aesar), hydrazine hydrate (Sigma Aldrich), 3,5 dichlorosalicylaldehyde, zinc acetate, copper acetate were of Analar grade and purchased from commercial sources. The solvents methanol (Spectrochem), acetonitrile (Spectrochem) and DMF (Spectrochem) were used without further purification.

2.2 | Synthesis of 3,5-dichlorosalicylaldehyde-N⁴-cyclohexyl thiosemicarbazone

The preparation of this compound involves a two-step process (shown in Schemes 1 and 2):

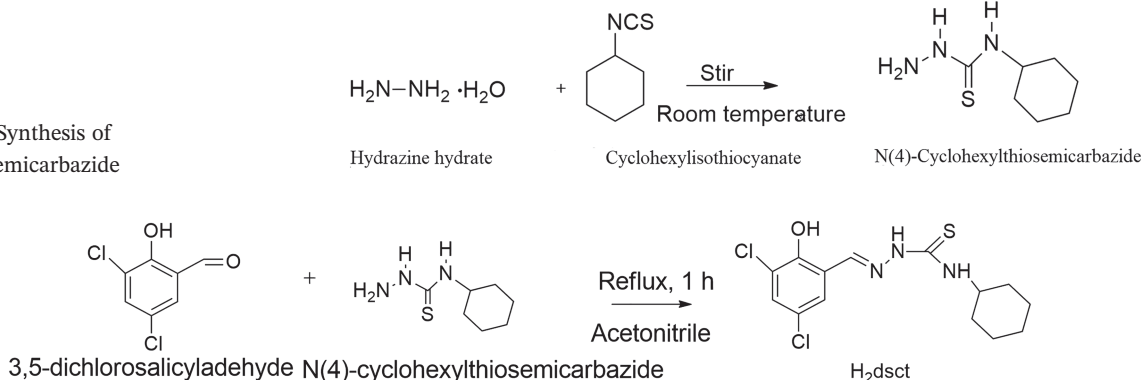
- Step 1.

Preparation of N⁴-cyclohexylthiosemicarbazide.

In the first step, cyclohexylisothiocyanate (2 ml, 15 mmol) in 20 ml methanol and hydrazine hydrate (4.3 ml, 90 mmol) in 20 ml methanol were mixed and the resulting solution was stirred. The resulting colourless product was filtered, washed with methanol and dried *in vacuo*.

- Step 2.

Synthesis of 3,5-dichlorosalicylaldehyde-N⁴-cyclohexylthiosemicarbazone (H₂dsct).

SCHEME 1 Synthesis of cyclohexylthiosemicarbazide**SCHEME 2** Synthesis of 3,5-dichlorosalicylaldehyde-N⁴-cyclohexylthiosemicarbazone

In the second step, 20 ml of acetonitrilic solution (15 ml) of N(4)-cyclohexylthiosemicarbazide (0.173 g, 1 mmol) was added to a solution of 3,5-dichlorosalicylaldehyde (0.191 g, 1 mmol) in 20 ml acetonitrile and the reaction mixture was refluxed for 1 hr after adding a drop of glacial acetic acid. The product was filtered, washed with acetonitrile and dried *in vacuo*. Yield: 0.1408 g (80%). ¹H-NMR (dms_o, δ ppm); 11.5 (1H,s), 8.3 (1H,s), 8.2 (1H,d), 7.9 (1H,s), 7.6 (1H,d), 4.2 (1H,t), 1.1–1.9 (1H,d); M.P.: 129 °C (Figure S1).

2.3 | Synthesis of metal complexes

2.3.1 | [Zn(dsct)(phen)]·DMF (1)

A methanolic solution of 1,10-phenanthroline (1 mmol, 0.198 g) was added to a hot solution of the H₂dsct (1 mmol, 0.340 g) with constant stirring which was followed by the addition of the zinc acetate (1 mmol, 0.219 g) in the solid form. The above dark green solution was refluxed for about 4 hrs and allowed to cool. It was kept aside for 1 week. Yellow colored crystals were formed on recrystallization from DMF. It was filtered, washed with methanol and dried *in vacuo*. Yield: 0.469 g (75%).

2.3.2 | [Zn(dsct)(bipy)]·DMF (2)

The complex [Zn(dsct)bipy]·DMF was prepared by refluxing a hot solution of H₂dsct and 2,2'-bipyridine (1 mmol, 0.156 g) in methanol-DMF mixture with methanolic solution of zinc acetate (1 mmol, 0.219 g) for 4 hrs. It was kept aside for slow evaporation for 1 week. The microcrystals obtained were separated and filtered. They were washed with methanol and finally dried *in vacuo*. Yield: 0.230 g (72%)

2.3.3 | [Cu(dsct)(bipy)]·DMF (3)

The thiosemicarbazone, H₂dsct (1 mmol, 0.346 g) was dissolved in methanol-DMF mixture and 2,2'-bipyridine (1 mmol, 0.156 g) in methanol was added to it. It was then followed by the addition of copper acetate (1 mmol, 0.199 g). The resulting solution was further refluxed for about 4 hrs and was then allowed to cool. Dark green crystals were formed over a period of 7 days, which was then washed with methanol and finally dried *in vacuo*. Yield: 0.248 g (78%)

2.4 | Physical measurements

Elemental (CHN) analysis were carried out using a Vario EL III CHNS analyser. Infrared spectra were recorded on a JASCO FT-IR-5300 Spectrometer in the 4000–400 cm⁻¹ range using KBr pellets. Electronic spectra were recorded on Thermo Scientific Evolution 220 model UV-visible spectrophotometer in the 200–1000 nm range using solutions in DMF. Molar conductivities of the complexes in DMF solutions (10⁻³ M) at room temperature were measured using a Systronic model 303 direct reading conductivity meter. ¹H NMR spectra of the thiosemicarbazone and its Zn (II) complexes were recorded using Bruker AMX 400 FT-NMR Spectrometer with DMSO-*d*₆ as the solvent and TMS as internal standard.

2.5 | X-ray crystallography

Single crystal of thiosemicarbazone and its complexes with suitable dimensions were selected and mounted on a Bruker SMART APEXII CCD diffractometer, equipped with a graphite crystal, incident-beam monochromator and a fine focus sealed tube with Mo K α ($\lambda = 0.71073 \text{ \AA}$) radiation as the X-ray source. The unit cell dimensions were measured and the data collection was performed at 292(2) K. The programs APEX2 and SAINT were used for

cell refinement and SAINT and XPREP were used for data reduction.^[22] Absorption corrections were carried out using SADABS based on Laue symmetry using equivalent reflections.^[23] The structures were solved by direct methods and refined by full-matrix least-squares refinement on F^2 using SHELXL-97 and SHELXL-2018/3^[24] provided in WinGX^[25]. The molecular and crystal structures were plotted using DIAMOND version 3.2 g^[26] and ORTEP.

In the H_2dsct and metal complexes, anisotropic refinement were performed for all non-hydrogen atoms and all H atoms on C were placed in calculated positions, guided by difference maps, with C–H bond distances 0.93–0.96 Å. H atoms were assigned as $U_{iso} = 1.2U_{eq}$ (1.5 for Me). In complexes **1** and **2**, the N3–H3' and N8–H8' H atoms were located from a difference map and their distances were restrained to 0.88 ± 0.01 Å.

In $[Zn(dsct)(phen)] \cdot DMF$ (**1**), the reflections (0 1 1), (0 1 0) and (3 3 7) were omitted due to bad agreement. In $[Zn(dsct)(bipy)] \cdot DMF$ (**2**), some of the reflections are omitted due to bad agreement. In $[Cu(dsct)(bipy)] \cdot DMF$ (**3**), the DMF molecule is disordered over two sites with 0.755(7) for the major and 0.245(7) for the minor occupied sites. The geometry of the minor disordered part was restrained to be planar by FLAT instruction. SIMU command has been given to restrain the atoms in the DMF molecule to be similar. The bond distances of the minor disordered DMF part was constrained to be similar to that of the major disordered part by SAME instruction. Some reflections in this complex was also omitted owing to bad agreement.

2.6 | Antibacterial activity

Antibacterial activities were screened *in vitro* against the following organisms, *E. coli*, *Salmonella typhi*, *Enterobacter aerogenes*, *Shigella dysenteriae*, *Bacillus cereus* and *Staphylococcus aureus*. The solutions of ampicillin (antibacterial drug) was used as standard drug. The disc agar diffusion method^[27] was employed for the determination of antimicrobial activities. 1 mg/ml of each complex is taken for the study. The compounds under investigation were dissolved in DMSO to a final concentration of 100 mg/ml. The antibacterial activity was compared with that of positive control of commercial and the most available drug, ampicillin. All the tests were performed in duplicate. The complex has good antimicrobial activity, if the inhibition zone measures ~2–3 mm and more effective if the inhibition zone is greater than 3 mm. If there is no inhibition zone, then the complex has no activity on the bacterium.^[28]

2.7 | Molecular docking studies

Cancer is the uncontrolled growth of abnormal cells. The epidermal growth factor (EGFR) is highly expressed in different types of cancers like colon, breast, and bladder cancers.^[29] Targeting this receptor is a good policy for the design of new anticancer drugs.^[30] Among the various cancers, breast cancer is one of the most recurring worldwide and deadliest cancers that have high number of mortality rates among females.

The key tool in computational drug design is molecular docking.^[31] The focus is to simulate the molecular recognition process. It aims to attain an optimized conformation for the drug and the protein with a relative orientation resulting in minimized overall free energy. In this paper, we used molecular docking of thiosemicarbazone (H_2dsct) and the two complexes with the ATP binding site of EGFR-TKs (1 m17)^[32] and breast cancer (3hb5)^[33] by Auto-Dock. Crystal Structure of PDB ID: 1 m17 and 3hb5 were obtained from protein data bank (<http://www.rcsb.org>). All bound water molecules were eliminated and the polar hydrogens were added. The ligand molecules in the cif format is converted to pdb format using mercury software.

2.8 | MTT assay

An *in vitro* cytotoxicity of the selected compound was tested by MTT assay method. Cells were placed in a 96 well tissue culture plate for 24 hrs incubation before adding complex, so as to allow attachment of cell to the wall of the plate. Non treated control cells were also maintained. After 24 hrs of incubation period, the sample content in wells were removed and 30 µl of reconstituted MTT solution was added to all test and cell control wells. The plate was gently shaken well and incubated at 37 °C in a humidified 5% CO₂ incubator for 4 hrs. After the incubation period, the supernatant was removed and 100 µl of MTT Solubilization Solution (DMSO) was added and the wells were mixed gently by pipetting up and down in order to solubilize the formazan crystals. The absorbance values were measured by using microplate reader at a wavelength of 540 nm.

The percentage of growth inhibition was calculated using the formula:

$$\% \text{ of viability} = \frac{\text{Mean OD Samples} \times 100}{\text{Mean OD of control group}}$$

3 | RESULTS AND DISCUSSION

A newly synthesized thiosemicarbazone and its three complexes were synthesized and characterized by elemental

analysis, molar conductivity measurements, IR, electronic and ^1H NMR spectral studies. The complexes were synthesized by refluxing an equimolar mixture of appropriate thiosemicarbazone with zinc/copper acetate along with the corresponding heterocyclic bases. Complexes **1** and **2** are yellow in colour whereas complex **3** is dark green in colour. In all the complexes, thiosemicarbazone exists in the thioiminolate form and act as a dideprotonated tridentate ligand coordinating through phenolic oxygen, thioiminolate sulfur and azomethine nitrogen. The metal complexes prepared are stable towards air and moisture at room temperature. They are insoluble in water but soluble in dipolar aprotic solvents like DMF and DMSO. On the basis of elemental analysis data, stoichiometry was assigned to the thiosemicarbazone and metal complexes, which was further confirmed by single crystal X-ray diffraction studies (Table S1). The molar conductivity measurements were measured in DMF (10^{-3} M) at room temperature for the H_2dsct and its metal complexes. The values were in the range $2\text{--}10 \Omega^{-1} \text{cm}^2 \text{mol}^{-1}$ suggesting that the complexes are non-electrolytic in nature and remain un-dissociated in DMF^[34].

3.1 | IR spectra

The characteristic IR bands of the complexes have shown significant changes as compared to that of the parent thiosemicarbazone and the shift of some of the characteristic vibrational frequency of the ligand upon complexation provides the mode of binding around the metal ion. The important IR frequencies of ligand and its complexes along with their relative assignments are given in Table S2. The infrared spectral data of the thiosemicarbazone derivative and complexes **1–3** are presented in the above table with their tentative assignments. The new band found at $\nu = 1596 \text{ cm}^{-1}$ is due to C=N bond resulting from enolization of the thiosemicarbazone ligand and the one at $\nu = 1509 \text{ cm}^{-1}$ is due to newly formed C=N of the thiosemicarbazone moiety upon complexation.^[35] Bands in the range $404\text{--}436 \text{ cm}^{-1}$ are assignable to $\nu(\text{M}\text{--}\text{N})$ frequencies.^[36] The decrease in the stretching frequency of C–S bond upon complexation indicates the coordination via its thiolate sulfur.

3.2 | Electronic spectra

The electronic spectrum of the H_2dsct was recorded in 10^{-5} M solution of DMF. The electronic spectra gave clear evidence of characteristic absorptions of aromatic groups as well as non-bonded electrons in the complex. The bands at 310 and 340 nm in the thiosemicarbazone derivative are due to $\pi \rightarrow \pi^*$ and $n \rightarrow \pi^*$ transitions.^[37] This

may be due to benzene ring, imine and thiocarbonyl groups present in the compound. These intraligand bands have undergone marginal changes during complexation. The spectra of these bands in complexes are found to be shifted in the region of 325–340 nm ($29,425 \text{ } \epsilon/\text{M}^{-1} \text{ cm}^{-1}$). In Zn complexes, the $\pi \rightarrow \pi^*$ bands are shifted to longer wavelength region as a result of the C–S bond being weakening and conjugation system enhancing on complexation.^[38] In addition to this, a new band in the range 390–410 nm ($17,340 \text{ } \epsilon/\text{M}^{-1} \text{ cm}^{-1}$) is observed for complexes which can be assigned to the $\text{O}_{\text{phenolate}}\text{--}\text{Zn}$, $\text{N}_{\text{azomethine}} \rightarrow \text{Zn}$ and $\text{S} \rightarrow \text{Zn}$ LMCT transitions.^[39,40]

But in $[\text{Cu}(\text{dsct})(\text{bipy})]\cdot\text{DMF}$ (**3**) absorptions in visible region in the 560–570 nm ($214 \text{ } \epsilon/\text{M}^{-1} \text{ cm}^{-1}$) range are attributable to $d\text{--}d$ transitions, as observed in many copper(II) complexes. In the Cu (II) complex, an intense band observed at 420 nm ($17304 \text{ } \epsilon/\text{M}^{-1} \text{ cm}^{-1}$) is assigned to ligand to metal charge transfer transition. The Cu(II) complexes with a square pyramidal geometry usually exhibits three spin allowed transitions; $\text{A}_{1g} \leftarrow \text{B}_{1g}$, $\text{B}_{2g} \leftarrow \text{B}_{1g}$ and $\text{E}_g \leftarrow \text{B}_{1g}$, but due to the very small energy difference between the d levels, the bands usually appeared are weak and overlapped, they become difficult to resolve them into separate components.^[40]

3.3 | Description of crystal structures

3.3.1 | Crystal structure of thiosemicarbazone

A colourless needle shaped crystals which are suitable for X-ray diffraction were obtained by the slow evaporation from a methanolic solution of the thiosemicarbazone. The compound crystallizes into a monoclinic $P2_1/c$ space group. The crystal data and structure refinement parameters are shown in Table 1. The ORTEP diagram for thiosemicarbazone is given in Figure 1. The condensation between aldehyde and thiosemicarbazide is evident from the azomethine bond, C(7)–N(1) bond length of 1.272(2), which is near to the reported C=N bond length (1.276(3) Å). The C(8)–S(1) bond length is 1.6781(19) Å and C(8)–N(2) bond length is 1.364(2) Å which are closer to the reported C=S and C–N bond lengths^[41]. These values suggested that the compound thiosemicarbazone exists in thio-amido form in the solid state. The *E* conformation of the compound with respect to C(7)–N(1) is derived from the torsion angle C(6)–C(7)–N(1)–N(2), $179.82(17)^\circ$. With respect to N(1), the thiol sulfur S(1) lies *trans* and N(3) lies *cis* which is.

evident from the N(1)–N(2)–C(8)–S(1) and N(1)–N(2)–C(8)–N(3) torsion angles $179.27(15)$ and $0.9(3)^\circ$

TABLE 1 Crystallographic data and structure refinement for H₂dsct, **1**, **2** and **3** complexes

Parameters	H ₂ dsct	[Zn(dsct)(phen)]·DMF (1)	[Zn(dsct)(bipy)]·DMF (2)	[Cu(dsct)(bipy)]·DMF (3)
Empirical formula	C ₁₄ H ₁₆ Cl ₂ N ₃ O S	C ₅₅ H ₅₃ Cl ₄ N ₁₁ O ₃ S ₂ Zn ₂	C ₂₇ H ₃₀ Cl ₂ N ₆ O ₂ SZn	C ₂₇ H ₂₉ Cl ₂ CuN ₆ O ₂ S
Formula weight	345.26	1252.74	638.92	636.06
Crystal system	Monoclinic	Triclinic	Triclinic	Monoclinic
Space group	<i>P</i> 2 ₁ / <i>c</i>	<i>P</i> $\bar{1}$	<i>P</i> $\bar{1}$	<i>P</i> 2 ₁ / <i>n</i>
Cell parameters				
a (Å)	14.3350(9)	10.6525(6)	11.9910(13)	16.0975(16)
b (Å)	6.1371(3)	9.8534(9)	16.209(2)	11.8316(10)
c (Å)	17.8397(11)	18.5996(10)	17.411(2)	17.5066(17)
α (°)	90	75.961(3)	62.524(5)	90
β (°)	93.154(3)	87.303(3)	87.233(6)	116.759(3)
γ (°)	90	73.516(3)	87.012(6)	90
Volume V (Å ³)	1567.08(16)	2761.3(3)	2997.2(6)	2977.2(5)
Z	4	2	4	4
Calculated density (ρ) (Mgm ⁻³)	1.459	1.507	1.416	1.419
Crystal size (mm ³)	0.300 x 0.250 x 0.250	0.350x0.300x0.300	0.35 x 0.30 x 0.30	0.35 x 0.30 x 0.30
θ range for data collection	2.759 to 28.310°	1.129 to 28.430°	1.319 to 28.347°	2.606 to 28.332°
Limiting indices	-19 ≤ h ≤ 19, -7 ≤ k ≤ 8, -23 ≤ l ≤ 23	-14 ≤ h ≤ 13, 20 ≤ k ≤ 20, 24 ≤ l ≤ 21	-15 ≤ h ≤ 16, 21 ≤ k ≤ 21, 22 ≤ l ≤ 23	-20 ≤ h ≤ 21, 12 ≤ k ≤ 15, 23 ≤ l ≤ 23
Reflections collected/Unique Reflections	18524/3893 [R (int) = 0.0311]	33530/13603 [R (int) = 0.0312]	21234/14988 [R (int) = 0.0383]	35415/7431 [R (int) = 0.0368]
Completeness to θ	25.242(99.9%)	25.242 (99.3%)	25.242 (97.2%)	25.242 (99.9%)
Maximum and Minimum transmission	0.872 and 0.844	0.8030 and 0.7740	0.8030 and 0.7740	0.7500 and 0.7180
Goodness-of-fit on F ²	1.012	0.986	0.966	1.074
Final R indices [<i>I</i> > 2 σ (<i>I</i>)]	R ₁ = 0.0393, wR ₂ = 0.1107	R ₁ = 0.0432, wR ₂ = 0.1107	R ₁ = 0.0654, wR ₂ = 0.1635	R ₁ = 0.0465, wR ₂ = 0.1133
R indices (all data)	R ₁ = 0.0551, wR ₂ = 0.1226	R ₁ = 0.0802, wR ₂ = 0.1320	R ₁ = 0.1512, wR ₂ = 0.2076	R ₁ = 0.0803, wR ₂ = 0.1387
Largest difference peak and hole (e Å ⁻³)	0.769 and 0.224	0.687 and - 0.638	0.842 and - 0.889	0.681 and - 0.445

$$R_1 = \frac{\sum ||F_o| - |F_c||}{\sum |F_o|}$$

$$wR_2 = \frac{[\sum w (F_o^2 - F_c^2)^2]}{\sum w (F_o^2)^2}^{1/2}$$

respectively. Selected bond lengths and bond angles of the thiosemicarbazone derivative and its complexes are given in Table 2.

The special packing of the thiosemicarbazone is assisted by the self-assembly of the molecules which is aided by the intramolecular hydrogen bonding which is shown in Figure S2 and C–H... π interactions which arranges the molecule in to a zig-zag manner in a unit cell (Table S3). The arrangement of atoms in the molecules give rise to only one intramolecular hydrogen bonding

N(2)–H(2)...O(1) with D–A distance of 3.024(2) Å (Table S2). The packing of molecules is further facilitated by C(3)–H(3)–Cg(1) interaction with H...Cg distance of 2.82 Å (Figure S3).

The asymmetric unit of [Zn(dsct)(phen)]·DMF (**1**), consists of two unique molecules, 1 and 2, with only slight differences in bond distances and angles between them. DMF molecule is present outside the coordination sphere (Figure 2). The structure of the complex shows that complexation was occurred by a thione to thiol tautomerism.

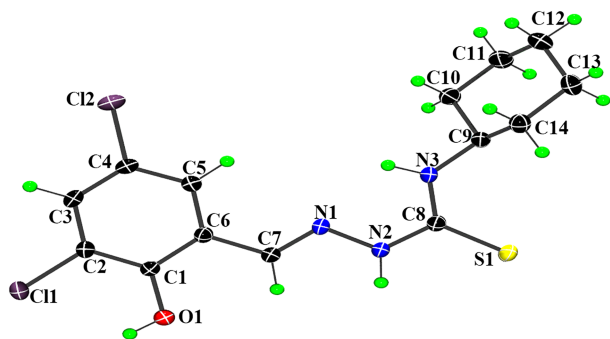


FIGURE 1 ORTEP representation showing the atom labelling of non-hydrogen atoms of the thiosemicarbazone (H_2dsct). Displacement ellipsoids are drawn at 30% probability

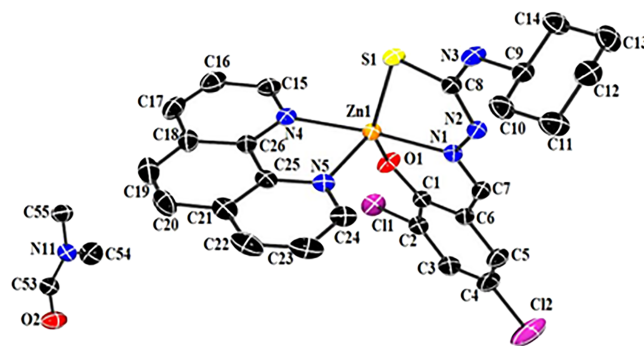


FIGURE 2 ORTEP representation showing the atom labelling of the complex $[Zn(dsct)(phen)] \cdot DMF(1)$

It is accompanied by double deprotonation of the thiol sulfur and hydroxyl oxygen atoms in the thiosemicarbazone. Therefore, it was doubly deprotonated and coordinated to

zinc *via* the imine nitrogen, the phenolic oxygen, thiolate sulfur atoms, and two nitrogen atoms of the 1,10-phenanthroline. To determine the degree of deviation from square pyramid or trigonal bipyramid geometry the

TABLE 2 Selected bond lengths (Å) and bond angles (°) of thiosemicarbazone and its complexes

Bond length (Å)							
H_2dsct		$[Zn(dsct)(phen)] \cdot DMF(1)$		$[Zn(dsct)(bipy)] \cdot DMF(2)$		$[Cu(dsct)(bipy)] \cdot DMF(3)$	
N(1)–N(2)	1.366(2)	N(1)–N(2)	1.383(3)	N(1)–N(2)	1.395(6)	N(1)–N(2)	1.405(3)
C(8)–S(1)	1.6781(19)	C(8)–S(1)	1.751(3)	C(8)–S(1)	1.755(5)	C(8)–S(1)	1.756(3)
C(7)–N(1)	1.272(2)	C(7)–N(1)	1.278(3)	C(7)–N(1)	1.282(6)	C(7)–N(1)	1.290(4)
C(8)–N(2)	1.364(2)	C(8)–N(2)	1.320(3)	C(8)–N(2)	1.291(7)	C(8)–N(2)	1.317(4)
		Zn(1)–N(1)	2.084(2)	N(1)–Zn(1)	2.084(4)	N(1)–Cu(1)	1.950(2)
		Zn(1)–N(4)	2.159(2)	N(4)–Zn(1)	2.106(4)	N(4)–Cu(1)	2.235(2)
		Zn(1)–N(5)	2.120(2)	N(5)–Zn(1)	2.123(4)	N(5)–Cu(1)	2.013(2)
Bond Angle (°)							
H_2dsct		$[Zn(dsct)(phen)] \cdot DMF(1)$		$[Zn(dsct)(bipy)] \cdot DMF(2)$		$[Cu(dsct)(bipy)] \cdot DMF(3)$	
C(7)–N(1)–N(2)	115.93(16)	C(7)–N(1)–N(2)	116.6(2)	C(7)–N(1)–N(2)	117.0(4)	C(7)–N(1)–N(2)	115.4(2)
C(8)–N(2)–N(1)	120.65(16)	C(8)–N(2)–N(1)	112.4(2)	C(8)–N(2)–N(1)	111.9(4)	C(8)–N(2)–N(1)	112.4(2)
C(8)–N(3)–C(9)	124.95(16)	C(8)–N(3)–C(9)	124.7(2)	C(8)–N(3)–C(9)	124.7(2)	C(8)–N(3)–C(9)	123.9(3)
N(3)–C(8)–N(2)	115.59(17)	N(2)–C(8)–N(3)	117.7(2)	N(2)–C(8)–N(3)	118.3(5)	N(2)–C(8)–N(3)	120.0(3)
N(3)–C(8)–S(1)	125.14(15)	N(3)–C(8)–S(1)	115.0(2)	N(3)–C(8)–S(1)	113.7(4)	N(3)–C(8)–S(1)	115.3(2)
N(2)–C(8)–S(1)	119.27(14)	N(2)–C(8)–S(1)	127.3(2)	N(2)–C(8)–S(1)	127.9(5)	N(2)–C(8)–S(1)	124.6(2)
		N(1)–Zn(1)–S(1)	82.26(6)	N(1)–Zn(1)–S(1)	81.45(13)	N(1)–Cu(1)–S(1)	84.45(7)
		N(1)–Zn(1)–N(4)	174.38(9)	N(1)–Zn(1)–N(4)	99.47(15)	N(1)–Cu(1)–N(4)	97.17(9)
		N(5)–Zn(1)–N(4)	78.15(9)	N(4)–Zn(1)–N(5)	77.46(15)	N(5)–Cu(1)–N(4)	77.28(8)
		N(4)–Zn(1)–S(1)	101.51(6)	N(4)–Zn(1)–S(1)	110.82(12)	N(4)–Cu(1)–S(1)	105.53(7)
		O(1)–Zn(1)–N(1)	89.10(8)	O(1)–Zn(1)–N(1)	89.46(16)	O(1)–Cu(1)–N(1)	93.48(9)
		O(1)–Zn(1)–N(5)	110.18(9)	O(1)–Zn(1)–N(5)	92.92(16)	O(1)–Cu(1)–N(5)	90.09(9)
		N(1)–Zn(1)–N(5)	96.67(9)	N(1)–Zn(1)–N(5)	176.66(16)	N(1)–Cu(1)–N(5)	174.00(9)
		O(1)–Zn(1)–N(4)	90.65(8)	O(1)–Zn(1)–N(4)	2.05(17)	O(1)–Cu(1)–N(4)	103.71(10)
		O(1)–Zn(1)–S(1)	139.15(7)	O(1)–Zn(1)–S(1)	137.07(13)	O(1)–Cu(1)–S(1)	150.72(8)
		N(5)–Zn(1)–S(1)	110.45(6)	N(5)–Zn(1)–S(1)	98.35(13)	N(5)–Cu(1)–S(1)	94.78(7)

trigonality index, $\tau = \frac{\beta - \alpha}{60}$, was calculated, wherein β and α are the two largest bond angles around the zinc atom.^[42]

For an ideal square pyramidal geometry $\tau = 0$ and for perfect trigonal bipyramidal geometry $\tau = 1$. The τ values found here are 0.5871 for Zn1 and 0.4236 in Zn2 indicate the irregular coordination geometry along the pathway of distortion to trigonal pyramidal. The non-linear trans bond angles, N(1)–Zn(1)–N(4) 174.38(9)°, N(5)–Zn(1)–S(1) 110.45(6)° and the bite angles N(4)–Zn(1)–S(1), 101.51(6)°, N(1)–Zn(1)–S(1), 82.26(6)°, O(1)–Zn(1)–N(1), 89.10(8)°, O(1)–Zn(1)–N(5), 110.18(9)°, N(5)–Zn(1)–N(4), 78.15(9)° also support the distorted geometry.

In this complex the ring puckering analysis and least square plane calculation show that the ring Cg(1), comprising of the atoms Zn(1), S(1), C(8), N(2) and N(1), is puckered with puckering amplitude $Q(2) = 0.3002 \text{ \AA}$ and $\Phi(2) = 359.4359^\circ$. Pseudorotation parameter P and τ_m of the five membered metalocycle was also calculated, and it was found that the metalocycle adopts envelope conformation with $P = 153.7^\circ$ and $\tau_m = 23.2^\circ$ for reference bond Zn(1)–S(1) in Cg(1) [32,33]. The ring Cg(3) and Cg(7), comprising of atoms Zn(1), O(1), C(1), C(6), C(7), N(1) in Cg(3) and C(9), C(10), C(11), C(12), C(13), C(14) in Cg(7) are also found to be puckered with puckering amplitude $Q = 0.3471 \text{ \AA}$, $\Theta = 115.80^\circ$ and $\Phi = 184.7091^\circ$ for Cg(3) and $Q = 0.5552 \text{ \AA}$, $\Theta = 0.72^\circ$ and $\Phi = 163.5292^\circ$ for Cg(7).

The molecules are connected in the crystal lattice by various intramolecular and intermolecular hydrogen bonding interactions (Table S3). These hydrogen-bonding interactions have considerable result upon the structural as well as spectral properties of the thiosemicarbazone

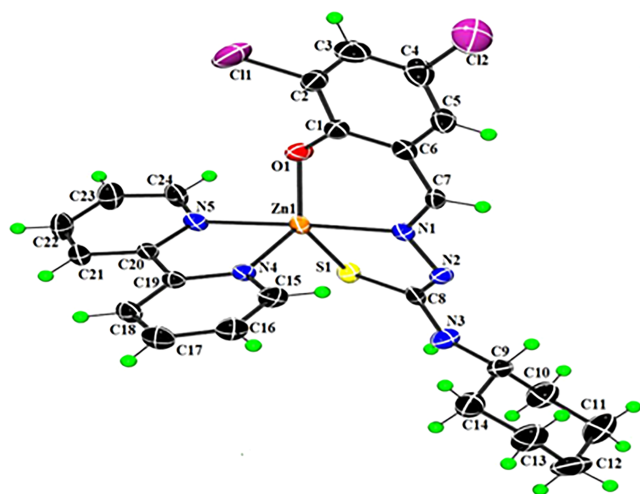


FIGURE 3 ORTEP representation showing the atom labelling of the complex $[\text{Zn}(\text{dsct})(\text{bipy})]\cdot\text{DMF}(2)$. DMF molecule has been omitted for clarity. Displacement ellipsoids are drawn at 30% probability

derivative (Figure S4). A significant $\pi\cdots\pi$ interactions strengthen the molecular chain by the interaction between the pyridyl ring and phenyl ring of two adjacent molecules with the centroid–centroid distances of 3.6355 \AA of the corresponding interacting rings which is shown in Figure S5.

The compound **2** is crystallized in triclinic $P\bar{1}$ space group. The molecular structure of crystal $[\text{Zn}(\text{dsct})(\text{bipy})]\cdot\text{DMF}$ (**2**) with atom numbering scheme is given in Figure 3. The asymmetric unit consist of two zinc (II) atom, two dianionic ligand moiety, two bipy and two DMF molecule. No lattice water molecule is present in the crystal system 3.

Each Zn(II) atom is five coordinated by one oxygen atom, one sulfur atom, one nitrogen atom from ligand moiety and two nitrogen atom from the bipyridine. The C–S bond length increases from 1.6781(19) \AA to 1.755(5) \AA in $[\text{Zn}(\text{dsct})\text{bipy}]\cdot\text{DMF}$ (**2**). After deprotonation the N2–C8 bond length also changes from 1.364(2) \AA to 1.291(7) \AA due to the enolization of the ligand for coordination.

For Zn1 the complex gives a value of $\tau = 0.659$ and for Zn2 a value of 0.649 for angular structural parameter, thereby confirming the distortion of the trigonal bipyramidal geometry in the complex. It is also evident from the bond angles $\text{N1–Zn1–N5} = 176.66(16)^\circ$, $\text{O1–Zn1–S1} = 137.07(13)^\circ$, $\text{N6–Zn2–N10} = 175.84(16)^\circ$, $\text{O2–Zn2–S2} = 136.90(13)$. Ring puckering analysis and least square plane calculations indicates that the ring Cg(1) consist of Zn(1), S(1), C(8), N(2), N(1) is found to be puckered with puckering amplitude $Q(2) = 0.4063 \text{ \AA}$, $\Phi(2) = 6.1637^\circ$. The puckering of the above five membered metalocycle was also calculated in terms of the pseudorotation parameter P and τ_m and it was found that the $P=166.5^\circ$ and $\tau=30.1^\circ$ for reference bond Zn(1)–S(1) in Cg(1) [39,40]. The Cg(3) comprising of O(1), C(1), C(6), C(7), N(1) and Cg(7) comprising of C(9),C(10), C(11), C(12), C(13), C(14) is also found to be puckered in the complex. The puckering amplitude $Q=0.2687\text{\AA}$, $\Theta=117.42^\circ$, $\Phi=203.8887^\circ$ for Cg(3) and $Q= 0.5732 \text{ \AA}$, $\Theta=178.35^\circ$, $\Phi=46.1687^\circ$ for Cg(7). Conformational analysis show that this metalocycle Cg (7) adopts the chair conformation.

The complex is driven by two classical hydrogen bonding interactions where the proton attached to N3' and N8' are involved in an intermolecular hydrogen bonding interactions with the O3 and O4 of the solvent molecule (Figure S6). Two important $\pi\cdots\pi$ interactions strengthen the molecular chain by the interaction between the bipyridyl rings of two adjacent molecules with the centroid–centroid distances of 3.7257 \AA and 3.7419 \AA of the corresponding interacting rings (Figure S7). Along with the $\pi\cdots\pi$ interaction, there are C–H $\cdots\pi$ interactions where the protons interact with the two six membered rings (Cg(6) and Cg(13)) (Table S6).

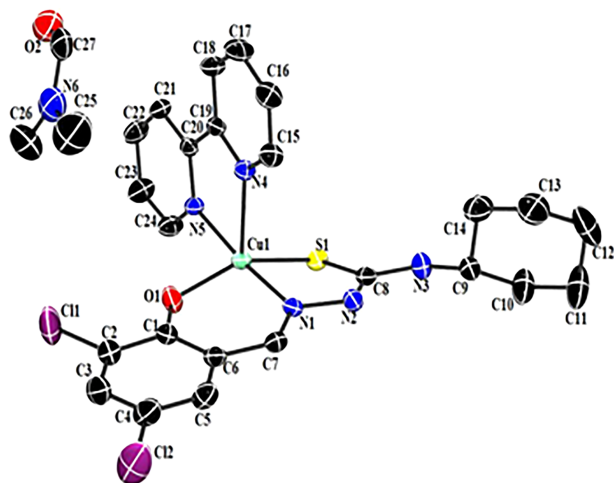
TABLE 3 Antibacterial activity of the complexes and standard ampicillin towards various bacteria

Bacteria	Zone of inhibition (mm)				
	H ₂ dsct	Complex 1	Complex 2	Complex 3	Ampicillin
<i>Escherichia coli</i>	4	8	4	8	7
<i>Salmonella typhi</i>	-	6	3	12	6
<i>Enterobacter aerogenes</i>	3	-	-	-	6
<i>Shigella dysenteriae</i>	2	-	-	-	12
<i>Bacillus cereus</i>	-	-	-	-	19
<i>Staphylococcus aureus</i>	-	-	-	-	17

TABLE 4 Docking interactions of the compound with 1m17 and 3hb5 proteins

Compound	Docking Score (kcal/mol)	Hydrogen bonding interactions	Electrostatic/hydrophobic interactions
<i>PDB ID: 1m17</i>			
H ₂ dsct	-7.0	ASP831	LEU820, LEU694, ALA719, VAL702, MET769
[Zn(dsdt)(bipy)]·DMF	-8.9	ASP831, S1-N5	LEU694, VAL702, ALA719, LYS721, CYS773, ARG817
[Cu([Cu(dsdt)(bipy)]·DMF	-9.6	-	ASP776, ASP831, PHE699, ALA719, MET769, LEU820, PHE699, CYS773, ARG817
<i>PDB ID: 3hb5</i>			
Ligand H ₂ dsct	-8.4	ASN152, TYR218	PHE192, PRO187, TYR155, VAL143, HIS221, VAL225, VAL196, MET193
[Zn(dsct)(bipy)]·DMF	-8.9	GLY92, S1-N5	ILE14, ALA91, ARG37, ALA191, PHE192, LEU93, VAL113
[Cu(dsct)(bipy)]·DMF	-8.9	ARG37, S1-N5	LYS195, LEU93, VAL196, PHE192, ALA191

The molecular structure of the compound, [Cu(dsct)(bipy)]·DMF (**3**) along with the atom numbering scheme is represented in Figure 4 and selected bond lengths and bond angles are summarized in Table 4. Suitable pale yellow crystals were obtained from recrystallization from

**FIGURE 4** ORTEP plot of [Cu(dsct)(bipy)]·DMF (**3**) along with atom numbering scheme of the non-hydrogen atoms. Displacement ellipsoids are drawn at 30% probability

DMF. The compound is monoclinic with $P2_1/n$ space group. It is a five coordinated mononuclear complex. DMF molecule is present outside the coordination sphere. The trigonality index $\tau = 0.38$ (where $\beta = \text{N}(1)\text{-Cu}(1)\text{-N}(5) = 174.00(9)^\circ$ and $\alpha = \text{O}(1)\text{-Cu}(1)\text{-S}(1) = 150.72(8)^\circ$). The differences in Cu-N bond distances $\text{N}(1)\text{-Cu}(1) = 1.950(2) \text{ \AA}$, $\text{N}(4)\text{-Cu}(1) = 2.235(2) \text{ \AA}$, $\text{N}(5)\text{-Cu}(1) = 2.013(2) \text{ \AA}$ indicate variations in the strengths of the bonds of coordinated nitrogen atoms. No classical hydrogen bonding is present in this compound. The various C-H bonds are forming hydrogen bonding with the sulfur and chlorine atom at a distances of 2.87, 2.92, 2.79 Å (Figure S8). There exist strong C-H \cdots π interactions between these metal containing chelate rings Cg(6) and Cg(3) with methyl protons and pyridyl ring protons (Table S7). Also significant C-H \cdots π interactions are observed with Cg(6) to the protons in the solvent molecule as well (Figure S9) 4

3.4 | Antimicrobial activity

The ligand (H₂dsct) and its metal complexes were screened against the bacterial strains *Escherichia coli*, *Salmonella typhi*, *Enterobacter aerogenes*, *Shigella dysenteriae*, *Bacillus*

cereus, *Staphylococcus aureus*. The zone of inhibitions are compared with standard antibacterial drug ampicillin. The results suggested that the complexes [Zn(dsct)(phen)]·DMF (**1**), [Zn(dsct)(bipy)]·DMF (**2**) and [Cu(dsct)(bipy)]·DMF (**3**) showed activity against *E. Coli* and *Salmonella typhi* whereas the ligand gave activity against *Escherichia coli*, *Enterobacter aerogenes*, *Salmonella typhi* and *Shigella dysenteriae*. The antimicrobial activity of H₂dsct ligand and its complexes is summarized in Table 3. Complexes **1** and **3** showed higher activity against bacterial strain, *Escherichia coli* than the reference drug (Ampicillin). Complex **3** showed remarkable activity against *Salmonella typhi* as compared to the standard drug. The minimum inhibitory concentration was evaluated by Muller Hinton broth method. It is the lowest concentration at which the complete inhibition of microorganism occurs. In this technique, different concentrations of complexes were inoculated with the bacterial culture which showed promising results. A positive control with culture and without complexes and a negative control without inoculating the culture but with complexes are maintained throughout. For H₂dsct, *Escherichia coli* gave 0.4 mg/ml, *Enterobacter aerogenes* gave 0.6 mg/ml and *Shigella dysenteriae* gave 0.9 mg/ml. For complexes **1**, **2** and **3**, *E. Coli* gives, 0.3, 0.4, 0.6 mg/ml respectively and *Salmonella typhi* gives, 0.4, 0.5, 0.8 mg/ml.

The azomethine (>C=N) group in the complexes have the potential to form hydrogen bonds with active centres within the cell that cause harm for the normal cell functioning and can lead to the killing of the bacteria or inhibiting their multiplication.^[43,44] The activity can be

explained on the basis of chelation theory^[45] which says that the increasing lipophilic nature of these complexes resulting from the metal chelation is responsible for the activity. In the chelate ring, the electron delocalization increases which increases the lipophilic character of the metal chelate. The antibacterial activity of complexes are also related to the existence of 1,10-phenanthroline and bipyridine as potential intercalator. The existence of such planar aromatic heterocycles impart the complexes with the opportunity to insert into the grooves of the double-helical DNA causing damage.^[46] The results from the complexes studied are consistent with those reported data for the biological activities in other copper(II) and zinc(II) complexes.^[47,48] Killing of the microbes or inhibiting their multiplication by blocking their active sites can be reasons for their antibacterial activity.

F5-F10

3.5 | Molecular docking studies

The thiosemicarbazone and the two complexes were evaluated for the inhibition of tyrosine kinase activity of EGFR and breast cancer mutant 3hb5-Oxidoreductase using the molecular docking method. Various interactions such as π -alkyl interaction, π - π interaction, π -donor hydrogen bond interaction and conventional hydrogen bond interaction through which ligands are binding to the protein molecule. The binding mode of compounds with the corresponding protein are shown in Figure 5–10. Docking interactions are given in Table 4.

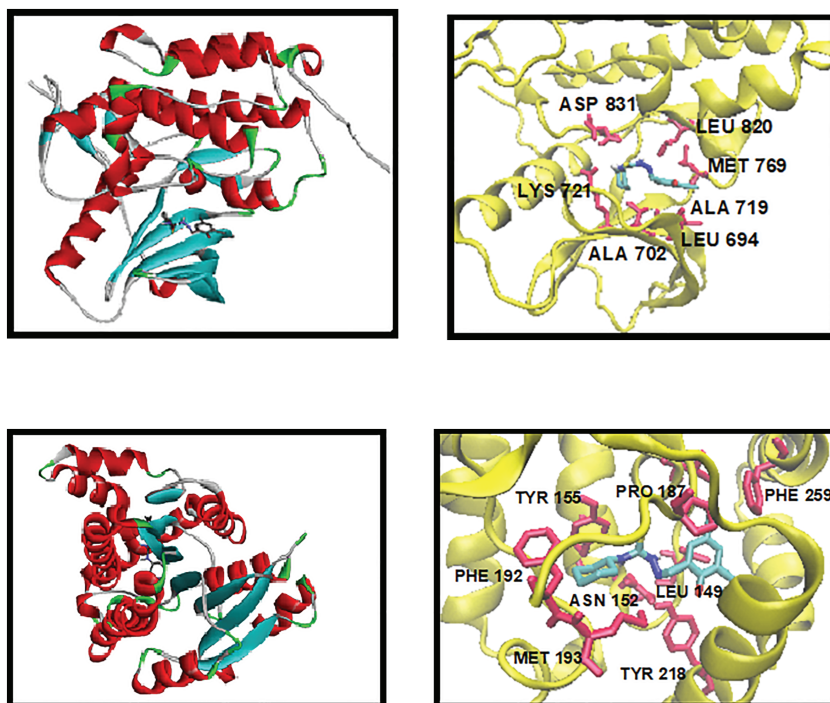


FIGURE 5 Interaction of 1 m17 on H₂dsct

FIGURE 6 Interaction of 1 m17 on [Zn(dsct)(bipy)]·DMF

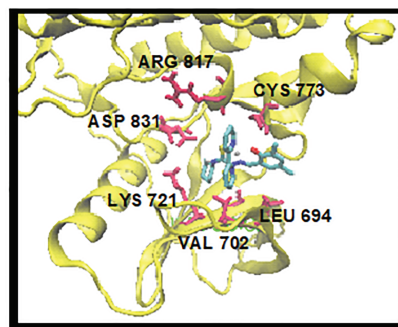
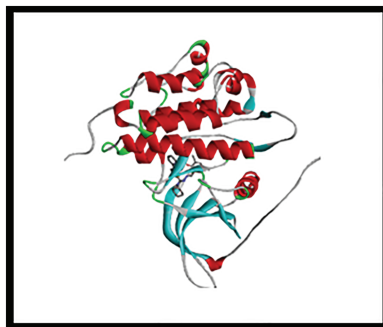


FIGURE 7 Interaction of 1 m17 on [Cu (dsc)(bipy)]•DMF

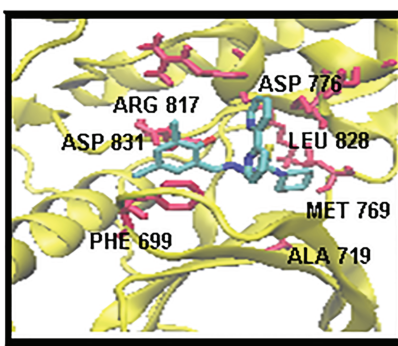
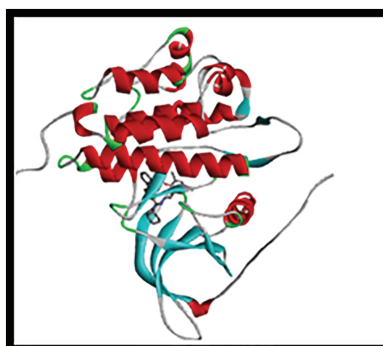


FIGURE 8 Interaction of 3hb5 on H₂dsc

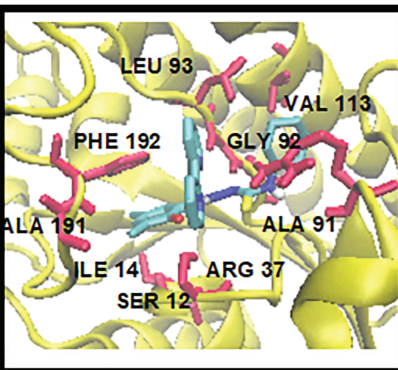
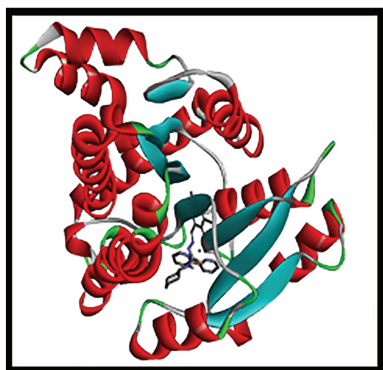


FIGURE 9 Interaction of 3hb5 on [Zn (dsc)(bipy)]•DMF

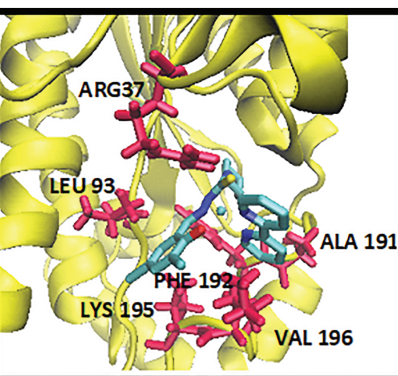
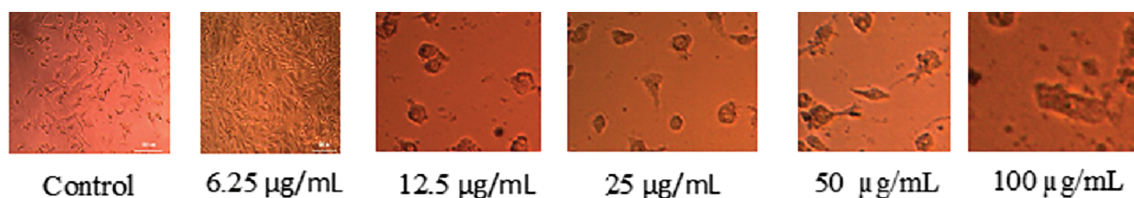


FIGURE 10 Interaction of 3hb5 on [Cu (dsc)(bipy)]•DMF

TABLE 5 In vitro cytotoxicity of Cu(II) complex against MCF-7 cancer cell line

Sample Concentration ($\mu\text{g/ml}$)	OD value I	OD value II	OD value III	Average OD	Percentage Viability
Control	0.8071	0.7936	0.7954	0.7987	100.00
6.25	0.3559	0.3562	0.3597	0.3573	44.73
12.5	0.2854	0.2836	0.2826	0.2839	35.54
25	0.1957	0.1983	0.1871	0.1937	24.25
50	0.1763	0.1711	0.1725	0.1733	21.70
100	0.1616	0.1606	0.1624	0.1615	20.22

**FIGURE 11** Phase contrast images

3.5.1 | Molecular docking analysis with 1 m17 protein

The synthesized thiosemicarbazone and the metal complexes were docked with 1 m17 tyrosine kinase protein. The thiosemicarbazone (H_2dsct) have formed one hydrogen bonding interaction with ASP831. The hydrogen bond was identified between NH of thiosemicarbazone and ASP831 and the distance was found to be 2.91 Å. The $[\text{Zn}(\text{dsct})(\text{bipy})]\cdot\text{DMF}$ (**2**) had formed two hydrogen bond interaction with ASP831 and a hydrogen bonding within the molecule. The first hydrogen atom is observed between OH of ASP831 with the C1–S1 bond of the complex and the distance was found to be 3.60 Å. The $[\text{Cu}(\text{dsct})(\text{bipy})]\cdot\text{DMF}$ (**3**) didn't show any hydrogen bond interaction with the active site of 1 m17 but the docking score is high indicating the importance of electrostatic and hydrophobic interactions shown by the compound with the active site of the protein. Among all the complexes synthesized, compound **3** showed highest docking score of -9.6 kcal/mol, which is higher than what is reported in literature.

3.5.2 | Molecular docking analysis with 3hb5 protein

The thiosemicarbazone (H_2dsct) has a better binding interaction with the breast cancer mutant 3hb5-oxidoreductase and in it exhibited binding energy of -8.4 kcal/mol along with 2 hydrogen bonding interactions. The first hydrogen bonding interaction is between

the OH of ASNX: 152 to the amino group of the thiosemicarbazone with 2.13 Å and the second hydrogen bonding interaction is between the oxygen of TYRX: 218 to the OH group of salicylaldehyde derivative. The compound $[\text{Zn}(\text{dsct})(\text{bipy})]\cdot\text{DMF}$ showed two hydrogen bond interaction with ASP831 and an intramolecular hydrogen bonding. The first hydrogen bond is between the NH of GLY92 with the N2 position of the compound with a distance of 2.31 Å and the other one is within the complex. In the $[\text{Cu}(\text{dsct})(\text{bipy})]\cdot\text{DMF}$ complex also there are two conventional hydrogen bond interactions present with ARG37 and an intramolecular hydrogen bonding. The distance of the interaction between ARG37 to the S1 of the compound is 2.81 Å. The results confirm that complex $[\text{Cu}(\text{dsct})(\text{bipy})]\cdot\text{DMF}$ showed efficient inhibition against 1 m17 and 3hb5 cancer cell lines and are having highest docking score as compared to reported ones. [49,50]

3.6 | Anticancer activity

Preparation of metal based anticancer drug is very important as they have proved to have anticancer activity. The compound $[\text{Cu}(\text{dsct})(\text{bipy})]\cdot\text{DMF}$ is screened for their anticancer activity against breast cancer cell line (MCF-7) at a concentration of 100 $\mu\text{g/ml}$. The LC_{50} values of the compound was measured by using different concentrations (5, 12.5, 25, 50 $\mu\text{g/ml}$). The complex showed an LC_{50} of 6.25 $\mu\text{g/ml}$. Furthermore, the compound was also screened against normal L929 (Mouse Fibroblast) cells line. The LC_{50} was found to be 218.338 $\mu\text{g/ml}$. Thus

the compound [Cu(dsct)(bipy)]·DMF, behaved as the most active and effective complex which can be used as an anticancer drug for breast cancer. The presence of azomethine group in the chelate ring may be the reason for its higher activity. When metal coordinated with the azomethine nitrogen in the chelate ring, the polarity reduces and increases the π -electron delocalization in the ligand moiety. Thus the entry through the lipid layer of cell membranes becomes more enhanced. The results can also be compared with literature, which shows that the compound is more efficient than what is reported already in the literature.^[51] (Table 5) (Figure 11)

4 | CONCLUSION

In this paper we have described the synthesis of zinc(II) and copper(II) complexes with an ONS donor thiosemicarbazone. The complexes were characterized by spectral studies. The molecular structures of H₂dsct, Zn(II) and Cu(II) complexes were confirmed by SCXRD analysis. In the complexes, thiosemicarbazone exists in the thioiminolate form and acts as dideprotonated tridentate ligands coordinating through phenolic oxygen, thioiminolate sulfur and azomethine nitrogen. In the analyzed complexes hydrogen bonding interactions and various nonbonding interactions played a principal role in the crystal network formation. The synthesized thiosemicarbazone and its complexes, had a satisfactory result for their antibacterial activity against bacterial species. All the complexes showed activity against bacterial strains *E.coli* and *Salmonella typhi*. The thiosemicarbazone showed activity against three bacterial strains such as *E. coli*, *Enterobacter aerogenes* and *Shigella dysenteriae*. Complex **2** showed very good activity as compared to standard drug (Ampicillin) against the bacterial strain, *Salmonella typhi*. Molecular docking acted as an additional tool for pharmacophore-based virtual screening to make the discovery of potent EGFR TK inhibitors and breast cancer mutant more efficient. Among the compounds that are screened, [Cu(dsct)(bipy)]·DMF gave very good docking score – 9.6 kcal/mol for 1 m17 cell line. [Cu(dsct)(bipy)]·DMF and [Zn(dsct)(bipy)]·DMF, both gave the same docking score of –8.9 kcal/mol for the 3hb5 cell line. The *in vitro* cytotoxic studies against breast cancer cell line (MCF-7) and normal L929 cell line revealed that the Cu(II) complex is a promising good anticancer agent and had the LC₅₀ of 6.25 μ g/ml. So the compound can be considered as important and effective drug against breast cancer. Thus the above study could be useful for the *in vivo* studies and can be the foundation stone for its applications in the field of drug development.

ACKNOWLEDGEMENTS

Nimya Ann Mathews acknowledges the University Grants Commission, New Delhi, India for the award of a Junior Research Fellowship. The authors are thankful to the Sophisticated Analytical Instrumentation Facility, Cochin University of Science and Technology, Kochi, India for elemental analyses, NMR spectra and single crystal X-ray diffraction measurements. They are also grateful to Biogenix Research Center, Thiruvananthapuram for anticancer activity studies.

ORCID

M.R. Prathapachandra Kurup  <https://orcid.org/0000-0002-9434-890X>

REFERENCES

- [1] (a) A. Ramdas, V. Sathish, M. Velayudham, P. Thanasekaran, K. L. Lu, S. Rajagopal, *Inorg. Chem. Commun.* **2013**, 35, 186. (b) C. R. Kowol, P. Heffeter, W. Miklos, L. Gille, R. Trondl, L. Cappellacci, W. Berger, B. K. Keppler, *J. Biol. Inorg. Chem.* **2012**, 17, 409. (c) J. Deng, G. Su, P. Chen, Y. Du, Y. Gou, Y. Liu, *Inorg. Chim. Acta* **2018**, 471, 194.
- [2] (a) N. S. Youssef, A. M. A. El-Seidy, M. Schiavoni, B. Castano, F. Ragaini, E. Gallo, A. Caselli, *J. Organomet. Chem.* **2012**, 714, 94. (b) J. Deng, T. Li, G. Su, Q. Qin, Y. Liu, Y. Gou, *J. Mol. Struct.* **2018**, 1167, 33.
- [3] T. S. Lobana, Rekha, R. J. Butcher, A. Castineiras, E. Bermejo, P. V. Bharatam, *Inorg. Chem.* **2006**, 45, 1535.
- [4] T. S. Lobana, P. Kumari, G. Hundal, R. J. Butcher, A. Castineiras, T. Akitsu, *Inorg. Chim. Acta* **2013**, 394, 605.
- [5] R. N. Prabhu, R. Ramesh, *Tetrahedron Lett.* **2013**, 54, 1120.
- [6] J. Haribabu, K. Jeyalakshmi, Y. Arun, N. S. P. Bhuvanesh, P. T. Perumal, R. Karvembu, *J. Biol. Inorg. Chem.* **2016**, 461.
- [7] M. Muralisankar, N. S. P. Bhuvanesh, A. Sreekanth, *New J. Chem.* **2016**, 40, 2661.
- [8] X. B. Yang, Q. Wang, Y. Huang, P. H. Fu, J. S. Zhang, R. Q. Zeng, *Inorg. Chem. Commun.* **2012**, 25, 55.
- [9] (a) A. Castineiras, N. F. Hermida, I. G. Santos, L. G. Rodriguez, *Dalton Trans.* **2012**, 41, 13486. (b) A. K. El-Sawaf, M. A. Azzam, A. M. Abdou, H. A. El, *Inorg. Chim. Acta* **2018**, 483, 116.
- [10] T. S. Lobana, S. Indoria, H. Sood, D. S. Arora, B. S. Randhawa, I. G.-Santos, V. A. Smoiniski, J. P. Jaisniski, *Inorg. Chim. Acta* **2017**, 461, 248.
- [11] M. Joseph, V. Suni, M. R. P. Kurup, E. Suresh, A. Kishore, S. G. Bhat, *Polyhedron* **2004**, 23, 3069.
- [12] R. A. Finch, M. C. Liu, A. H. Cory, J. G. Cory, A. C. Sartorelli, *Adv. Enzyme Regul.* **2000**, 39, 3.
- [13] A. M. Traynor, J. W. Lee, G. K. Bayer, J. M. Tate, S. P. Thomas, M. Mazurczak, D. L. Graham, J. M. Kolesar, J. H. A. Schiller, *Invest. New Drugs* **2010**, 28, 91.
- [14] (a) J. Sorenson, *Curr. Med. Chem.* **2002**, 9, 639. (b) S. Indoria, T. S. Lobana, H. Sood, D. S. Arora, G. Hundal, J. P. Jasinski, *New J. Chem.* **2016**, 40, 3642. (c) J. Deng, P. Yu, Z. Zhang, J. Wang, J.

- Cai, N. Wu, H. Sun, H. Liang, F. Yang, *Eur. J. Med. Chem.* **2018**, *158*, 442.
- [15] M. A. Hussein, T. S. Guan, R. A. Haque, M. B. K. Ahamed, A. M. S. A. Majid, *Polyhedron* **2015**, *85*, 93.
- [16] C. Umadevi, P. Kalaivani, H. Pushmann, S. Murugan, P. S. Mohan, R. Prabhakaran, *J. Photobiol. Photochem.* **2017**, *B 67*, 45.
- [17] G. Kalairasi, R. Jain, H. Pushman, S. P. Chandrika, K. Preethi, R. Prabhakaran, *New J. Chem.* **2017**, *41*, 2543.
- [18] G. Kalairasi, R. Jain, A. Shanmugapriya, H. Pushman, P. Kalaivani, R. Prabhakaran, *Inorg. Chim. Acta* **2017**, *462*, 174.
- [19] G. Zhao, H. Lin, *Curr. Med. Chem.* **2005**, *5*, 137.
- [20] P. U. Maheswari, S. Roy, H. D. Dulk, S. Barends, G. V. Wezel, B. Kozlevcar, P. Gamez, J. Reedijk, *J. Am. Chem. Soc.* **2006**, *128*, 710.
- [21] (a) R. Loganathan, S. Ramakrishnan, E. Suresh, A. Riyasdeen, M. A. Akbarsha, M. Palaniandavar, *Inorg. Chem.* **2012**, *51*, 5512; (b) B. Maity, M. Roy, B. Banik, R. Majumdar, R. R. Dighe, A. R. Chakravarty, *Organometallics* **2010**, *29*, 3632. (c) S. T. Von, H. L. Seng, H. B. Lee, S. W. Ng, Y. Kitamura, M. Chikira, C. H. Ng, *J. Biol. Inorg. Chem.* **2012**, *17*, 57.
- [22] Bruker, *SMART and SAINT*, Bruker AXS Inc., Madison **1997**.
- [23] Bruker, *SADABS*, Bruker AXS Inc., Madison **1997**.
- [24] G. M. Sheldrick, *Acta Cryst* **2015**, *C71*, 3.
- [25] L. J. Farrugia, *J. Appl. Cryst.* **2012**, *45*, 849.
- [26] K. Brandenburg, *Diamond Version 3.2g*, Crystal Impact GbR, Bonn Germany **2010**.
- [27] D. C. Gross, J. E. De Vay, *Plant. Pathol.* **1977**, *11*, 13.
- [28] C. J. Dhanaraj, M. S. Nair, *Eur. Polym. J.* **2009**, *45*, 565.
- [29] W. J. Gullick, *Br Med Bull* **1991**, *47*, 87.
- [30] M. A. Abdelgawad, A. Belal, H. A. Omar, L. Hegazy, M. E. Rateb, *Arc. Pharm.* **2013**, *346*, 534.
- [31] (a) A. Beteringhe, C. Racuciu, C. Balan, E. Stoican, L. Patron, *Adv. Mater. Res.* **2013**, *787*, 236. (b) N. M. Hosny, M. A. Hussien, F. M. Radwan, N. Nawar, *Spectrochim. Acta* **2014**, *A13*, 121.
- [32] G. Banupriya, R. Sribalan, V. Padmini, *J. Mol. Struct.* **2018**, *1155*, 90.
- [33] A. A. El-Bindary, M. A. Hussein, R. A. El-Boz, *J. Mol. Liq.* **2015**, *211*, 256.
- [34] W. J. Geary, *Coord. Chem. Rev.* **1971**, *7*, 81.
- [35] A. Sreekanth, M. R. P. Kurup, *Polyhedron* **2003**, *22*, 3321.
- [36] (a) L. Latheef, E. Manoj, M. R. P. Kurup, *Polyhedron* **2007**, *26*, 4107. (b) M. R. P. Kurup, B. Varghese, M. Sithambaresan, S. Krishnan, S. R. Sheeja, *Polyhedron* **2011**, *30*, 70.
- [37] B. S. Garg, M. R. P. Kurup, S. K. Jain, Y. K. Bhoon, *Transition Met. Chem.* **1991**, *16*, 111.
- [38] V. Philip, V. Suni, M. R. P. Kurup, *Polyhedron* **2006**, *25*, 1931.
- [39] A. Sreekanth, S. Sivakumar, M. R. P. Kurup, *J. Mol. Struct.* **2003**, *47*, 655.
- [40] V. Philip, V. Suni, M. R. P. Kurup, M. Nethaji, *Polyhedron* **2005**, *4*, 1133.
- [41] E. B. Seena, M. R. P. Kurup, E. Suresh, *J. Chem. Crystallogr.* **2008**, *38*, 93.
- [42] A. W. Addison, T. N. Rao, J. Reedijk, J. Van Rijn, G. C. Verschoor, *J. Chem. Soc. Dalton Trans.* **1984**, 1349.
- [43] (a) P. P. Netalkar, S. P. Netalkar, V. K. Revankar, *Polyhedron* **2015**, *100*, 215. (b) N. A. Mathews, A. Jose, M. R. P. Kurup, *J. Mol. Struct.* **2019**, *1178*, 544.
- [44] E. B. Anderson, T. E. Long, *Polymer* **2010**, *51*, 2447.
- [45] B. Tweedy, *Phytopathology* **1964**, *55*, 910.
- [46] (a) K. E. Erkkila, D. T. Odom, J. K. Barton, *Chem. Rev.* **1999**, *99*, 2777. (b) L.-N. Ji, X.-H. Zou, J.-G. Liu, *Coord. Chem. Rev.* **2001**, *216*, 513.
- [47] R. P. John, A. Sreekanth, V. Rajakannan, T. A. Ajith, M. R. P. Kurup, *Polyhedron* **1999**, *23*, 2459.
- [48] R. Fekri, M. Salehi, A. Asadi, M. Kubicki, *Applied Organomet.* **2017**, 4019.
- [49] G. Banupriya, R. Sribalan, V. Padmini, *J. of Mol. Struct.* **2018**, *1155*, 90.
- [50] N. Hassan, A. Z. El-Sonbati, M. G. El-Desouky, *J. Mol. Liq.* **2017**, *242*, 293.
- [51] W. H. Mahmoud, R. G. Deghadi, M. M. E. L. Desssouky, G. G. Mohamed, *Applied Organomet.* **2019**, *33*, 4556.

SUPPORTING INFORMATION

Additional supporting information may be found online in the Supporting Information section at the end of the article.

How to cite this article: Mathews NA, Begum PMS, Kurup MRP. Synthesis, characterization, biological screening and molecular docking of Zn (II) and Cu(II) complexes of 3,5-dichlorosalicylaldehyde-N⁴-cyclohexylthiosemicarbazone. *Appl Organometal Chem.* 2019;e5294. <https://doi.org/10.1002/aoc.5294>